

Spatial Uniformity Evaluation of Atmospheric-Pressure Microwave Line Plasma for Wide-Area Surface Treatment^{*)}

Haruka SUZUKI^{1,2)}, Hirotsugu KOMA¹⁾, Tomohiro OGASAWARA¹⁾, Yosuke KOIKE¹⁾
and Hirotaka Toyoda^{1,2,3)}

¹⁾*Department of Electronics, Nagoya University, Furo-cho, Chikusa-ku, Nagoya 464-8603, Japan*

²⁾*Center for Low-temperature Plasma Sciences, Nagoya University, Furo-cho, Chikusa-ku, Nagoya 464-8603, Japan*

³⁾*National Institute for Fusion Science, 322-6 Oroshi, Toki 509-5292, Japan*

(Received 17 October 2020 / Accepted 13 February 2021)

Spatial uniformity of an atmospheric-pressure microwave line plasma is evaluated from surface hydrophilicity treatment of polyethylene terephthalate film as well as observation of optical emission from the plasma. Prior to the experiments, the structure of the waveguide-based plasma source is optimized using a three-dimensional electromagnetic simulation to suppress standing-wave generation for the uniformity of plasma production. The spatial distribution in the longitudinal direction of the Argon (Ar) plasma is investigated by operating the microscope parallel to the slot and by irradiating film with the plasma to improve surface wettability of the film. Uniform profile of water contact angle is obtained in 40 cm with very high-speed processing.

© 2021 The Japan Society of Plasma Science and Nuclear Fusion Research

Keywords: atmospheric pressure plasma, microwave plasma, hydrophilic treatment of film

DOI: 10.1585/pfr.16.1406046

1. Introduction

The increased demand for electronic products has been the driving force behind the development of advanced atmospheric-pressure plasma techniques for low-cost and high-speed processing of surface area treatment, such as cleaning, modification [1–7], and film deposition [8–12]. Such surface area treatment applications require spatially uniform, high-density, and large-scale atmospheric-pressure plasma sources. So far, various types of atmospheric-pressure plasmas, such as dielectric barrier discharge (DBD) [13, 14], RF discharge [15, 16], and pulsed DC discharge [17] have been proposed. However, these plasma sources often do not meet the required specifications because the plasma density is not uniform in space and has a low density. This is caused by spatiotemporally intermittent discharges.

Atmospheric-pressure microwave plasma (APMP) sources are alternative promising candidates for high-density plasma sources because they can easily produce high-density plasma [18–22]. However, APMPs are rather difficult to match large-area processing because they have a short microwave wavelength ranging between a few to tens centimeters. This easily generates standing waves resulting in spatially non-uniform discharges. To solve this issue, we have developed a slotted-waveguide-based microwave plasma source, which we call atmospheric-pressure microwave line plasma (APMLP), that uses travelling waves and do not generate standing waves inside

the waveguide. So far, we reported the production of atmospheric-pressure plasma using rare-gas discharges in the meter-scale slot [23, 24]. Furthermore, we successfully produced N₂ molecular gas plasma of about 30 cm by flattening the cross-sectional structure of the waveguide, namely the low-impedance waveguide, to increase the electromagnetic field density [25]. Alternatively, the electromagnetic field was further increased by modifying the cross-sectional structure of the rectangular waveguide, turning it from symmetric to non-symmetric. To suppress standing-wave generation between the asymmetric structure waveguide and the standard waveguide, we designed an impedance matcher using three-dimensional electromagnetic field simulations. Consequently, we succeeded in producing the molecular gas plasma production on a meter scale [26]. APMLP has a unique characteristic: it is one meter long in the longitudinal direction and extremely narrow (0.1 mm) in the width direction. In our previous work, the longitudinal spatial uniformity of the emission intensity, plasma density, and gas temperature was confirmed *macroscopically* by taking the overall information and averaging the emission intensity across the slot width direction. However, we have not observed the detailed plasma structure in the slot width direction as well as the spatial uniformity of the electromagnetic field distribution in the asymmetric waveguide. It was rather difficult to measure such a narrow-gap plasma using our conventional setup.

In this study, we explore the structure of the impedance matching unit between the asymmetric and the standard waveguides using an electromagnetic simulator

author's e-mail: hsuzuki@nuee.nagoya-u.ac.jp

^{*)} This article is based on the invited talk at the 35th JSPF Annual Meeting (2018, Osaka).

for further optimization. We investigate the spatial homogeneity of the electromagnetic field distribution. Using optical microscopy, the emission intensity distribution in the slot width direction and the longitudinal direction is investigated. This activity enabled us to demonstrate the spatial uniformity of the plasma in the longitudinal direction. Furthermore, a polyethylene terephthalate (PET) resin film is irradiated with plasma and then we evaluated the spatial variation of the water contact angle and its treatment speed.

2. Atmospheric-Pressure Microwave Line Plasma

Figure 1 shows a schematic view of the atmospheric-pressure microwave line plasma (APMLP). This plasma source utilizes one-directional microwave power flow through a waveguide, which can be realized by using a looped waveguide with a circulator [23, 24] or a power absorber at the end of the waveguide. In this study, the power absorber has been used to absorb surplus of input microwave power (2.45 GHz, <1 kW) from a magnetron. A long slot (length: 110 cm, gap width: 0.12 mm) is placed on the waveguide (length: 1.2 m) and plasma is produced by the electric field induced in the slot. The suppression of standing-wave generation in the waveguide leads to the production of one-dimensional very long APP. To ease the APP production, the electric field in the slot was enhanced by modifying the waveguide from a rectangular cross-section (96 mm × 27 mm) into an asymmetric cross-section as shown in Fig. 2 [26]. In the modified part of the waveguide, a metal block (width: 34 mm, height: 22 mm) is placed on one side of the waveguide. Ar gas (<14 slm) was introduced in the waveguide. Air-tight windows are placed at both ends of the waveguide and the Ar gas flowed

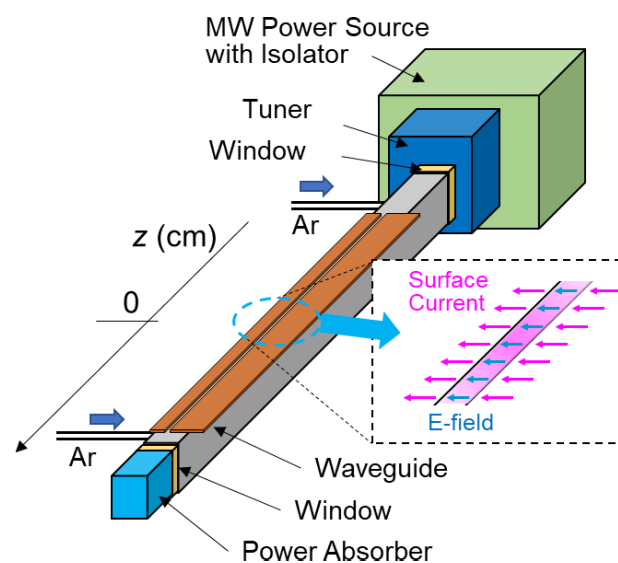


Fig. 1 Schematic view of atmospheric-pressure microwave line plasma (APMLP).

out through the slot to the atmosphere.

Since the waveguide with the modified cross-section is used for plasma production, the use of an impedance matching unit between the rectangular waveguide and the modified waveguide is critical for suppressing the power reflection at the connection between the waveguides. In this study, an impedance matching unit of a step-like structure was adopted (Fig. 2) and optimum structure was explored by using the commercially available electromagnetic simulation software MW-Studio. The simulations are based on finite-integration methods. A wave packet is introduced to a modeled waveguide structure and time development of the microwave in the waveguide is calculated. The measurement result is converted into the frequency domain and spatial profile of the microwave field at a target frequency (2.45 GHz). The *S* parameters of the waveguide are also obtained. Figure 3 (a) shows two examples of simulated electric field intensities along the modified waveguide at $x = 25$ mm and $y = 41$ mm, with two different step height (a) and step length (b) combinations: (i) $a = 16.0$ mm, $b = 39.5$ mm; and (ii) $a = 16.7$ mm, $b = 40.1$ mm. In both cases, the input power is normalized at 1 W. This figure demonstrates strong electric fields at the position of the impedance matching unit because of multi-reflection that takes place inside the matching unit. In the modified waveguide, a standing wave is observed along the waveguide in the case (i). However, standing wave is suppressed in the case (ii), showing the effectiveness of the step-like impedance matching unit. Figure 3 (b) shows the simulated peak-to-peak electric fields in the modified waveguide with various combinations of a and b . Results confirm that the condition (ii) is the optimized condition.

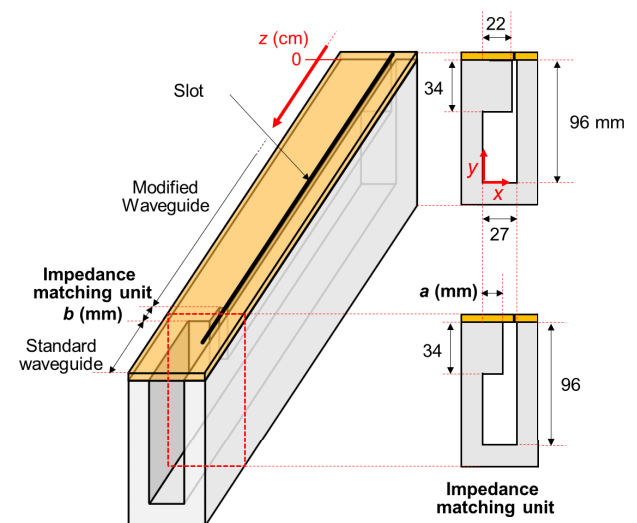


Fig. 2 Asymmetric cross-section waveguide with impedance matching units.

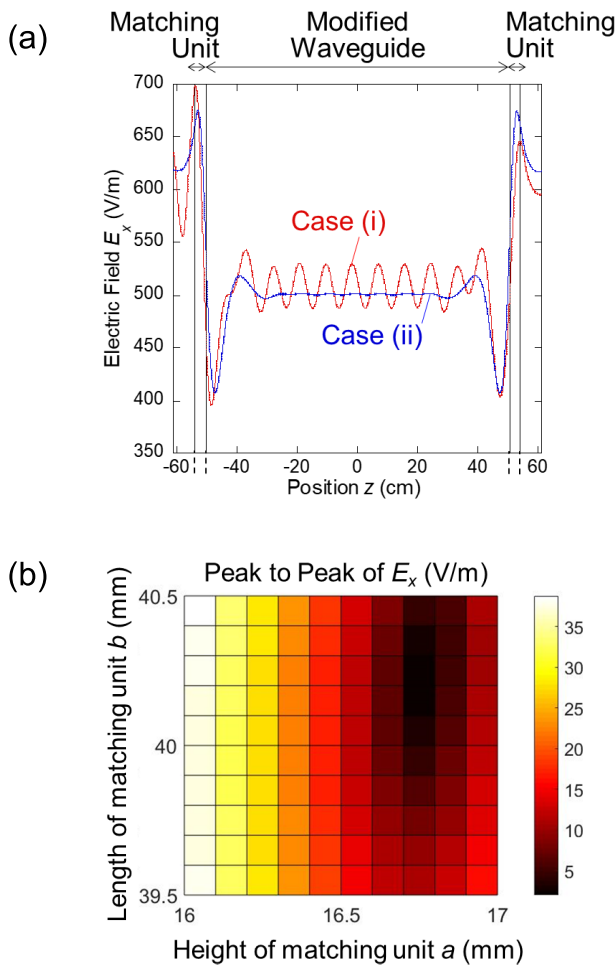


Fig. 3 Simulated results of (a) electric field intensity along the modified waveguide at $x = 25$ mm and $y = 41$ mm, and (b) peak-to-peak voltage in the modified waveguide with various combinations of a and b .

3. Microscopic Observation of Plasma Emission from APMLP

So far, we confirmed the longitudinal plasma uniformity of APMLP of 110 cm in length using a digital camera that was placed 1.5 m away from the plasma. However, in this experiment, the uniformity in the longitudinal direction was confirmed only by the integrated emission intensity across the slot gap as the camera does not have such a high spatial resolution. To confirm the uniformity of the plasma in the longitudinal direction, the plasma structure across the sub-mm gap slot should be the same independently of the longitudinal position of the meter-sized APMLP. To evaluate this, optical measurements using a rail-guided microscope with a digital camera was carried out. A schematic of the experimental setup is shown in Fig. 4. An optical bench was installed in parallel with the waveguide and a digital camera with a microscope (magnification factor: 20) moves along the slot. The camera was focused on the surface of the slot plates and the emission profile across the slot was investigated in the range of

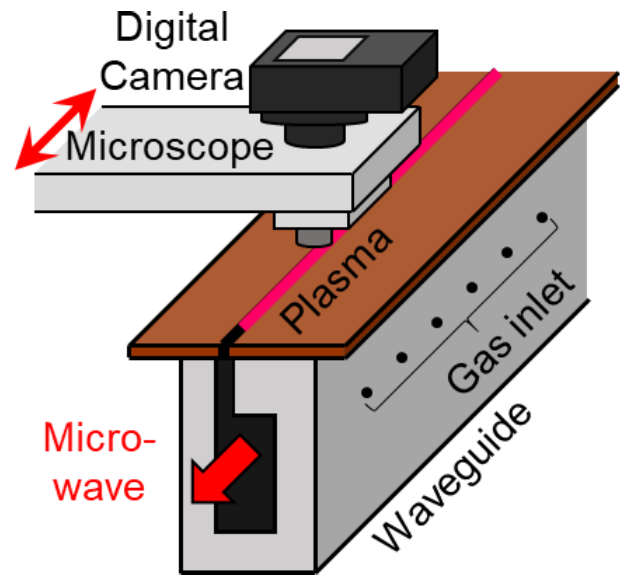


Fig. 4 Schematic image of the experimental setup for microscopic observation of plasma emission from APMLP.

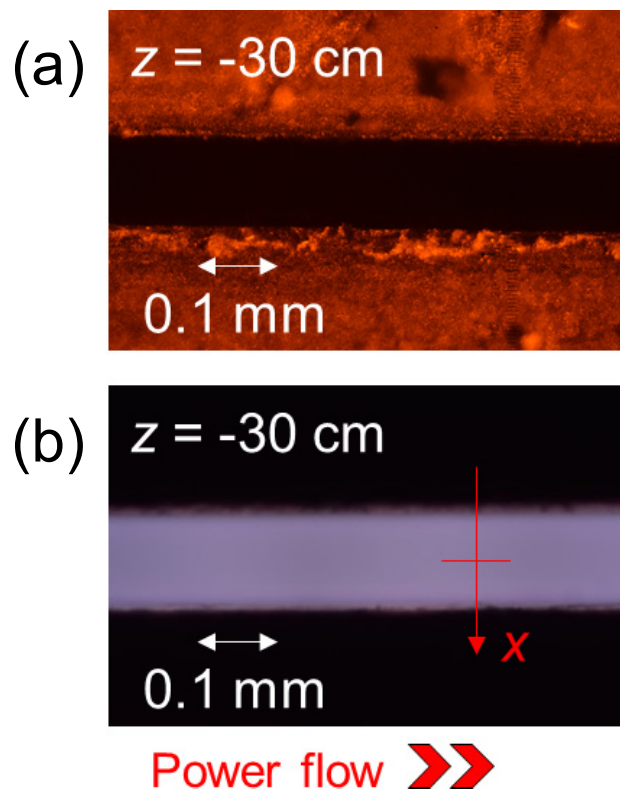


Fig. 5 Observed images of (a) the slot without plasma production at $z = -30$ cm, (b) plasma emission in the slot at $z = -30$ cm.

$z < \pm 30$ cm from the slot center.

Figure 5(a) shows an example of a slot image without plasma production at $z = -30$ cm. By taking photographs at different positions along the z axis, the accuracy of the slot width along the longitudinal direction is

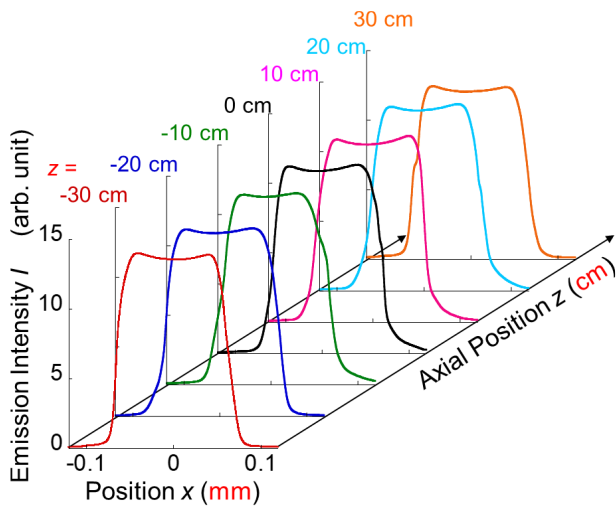


Fig. 6 Emission intensity profiles across the slot gap from $z = -30$ cm to $z = +30$ cm.

confirmed to be 0.12 mm with a deviation of less than 5%. Using this slot configuration, meter-sized plasma was successfully produced at an Ar flow rate of 14 slm and with a microwave power of 900 W. Figure 5 (b) shows an image of plasma emission in the slot at the same position as that of Fig. 5 (a). The exposure time of the camera is 1/40 s. The figure shows the emission intensity in the vicinity of the slot edge is slightly higher compared with that in the middle of the gap.

From similar photograph as that of Fig. 5 (b) in different z positions from $z = -30$ to $+30$ cm, emission intensity profiles across the slot gap (red line in Fig. 5 (b)) are obtained by processing the photograph data, as shown in Fig. 6. Please note that the horizontal axis is in the scale of 0.1 mm although the variation in the z axis is 60 cm. The emission profile in the slot (x -axis), especially in the vicinity of the plates at $x = -0.06$ mm and $x = +0.06$ mm, varies slightly in the z axis due to slightly out-of-focus image, but the result shows that the plasma structure across the slot is almost similar along the plasma length of 60 cm. Figure 7 shows the z position dependence on the emission intensity at the gap center. The emission intensity is slightly high at the upstream side of the microwave power flow. However, the difference of the emission intensity at $z = -30$ cm and $z = +30$ cm is within 6%. These results confirm that one-dimensional uniform plasma is produced along the slot with a length of 60 cm. We have monitored microwave power flow at the upstream and downstream sides by a microwave power monitor; the microwave power at the downstream side is around 600 W. Taking the uniform plasma production with a plasma length of 60 cm into account, the microwave power absorption at unit length (1 cm) is estimated to be around 5 W/cm.

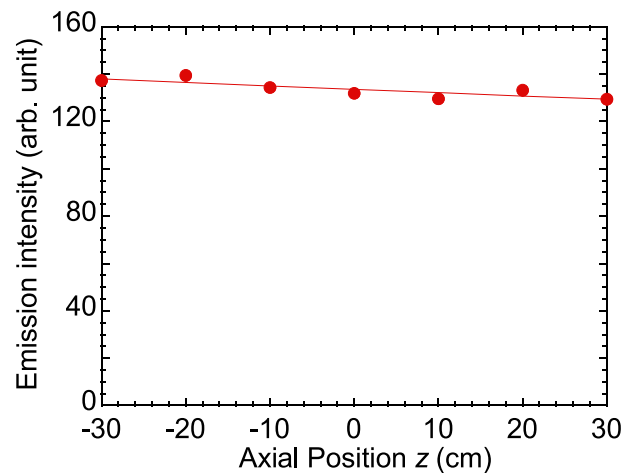


Fig. 7 Axial position z dependence of the emission intensity at the center of the gap.

4. Hydrophilic Treatment of PET Film

A typical application of APP is surface wettability control. To demonstrate the ability of the APMPLP for use in the treatment of a large surface area, a substrate scanning stage (width: 1 m, length: 50 cm, scanning distance 80 cm, scan speed: <10 m/min) was constructed and the APMPLP was placed on the scanning stage. The distance between the PET samples and the slot was 1.5 mm. To examine the surface treatment uniformity of this plasma source, PET films (width: 2 cm, length: 5 cm, and thickness: $100\ \mu\text{m}$) were placed at equal distances of 10 cm both in z and x axes as shown in Fig. 8. In the experiment, the slot width was 0.12 mm, whereas the input power was 900 W. Pure Ar at a flow rate of 28 slm was introduced into the waveguide from 16 gas inlets through a gas manifold behind the waveguide. This design improves gas flow uniformity and the process uniformity along the longitudinal direction of the slot. Samples were scanned in the x -axis at a scanning speed of 2 m/min.

Figure 9 shows the water contact angle of the PET film after Ar plasma treatment. The water contact angle is around 45° and is almost uniform both in x and z axes. It is known that the water contact angle decreases with the process time and saturates to a minimum value after a certain process time. We have confirmed that the initial and saturated water contact angles are $74\pm 2^\circ$ and $35\pm 2^\circ$ in our plasma source, respectively. The results of Fig. 9 show that the water contact angle is not saturated at a scanning speed of 2 m/min in the x -axis. This shows that the uniformity is not obtained by the saturation of the contact angle but by the uniformity of the plasma. Furthermore, the plasma is temporally stable and spatially uniform in the x and z axes, respectively. This result indicates the potential of APMPLP in two-dimensional large-area surface treatment.

To evaluate the hydrophilic treatment with respect to

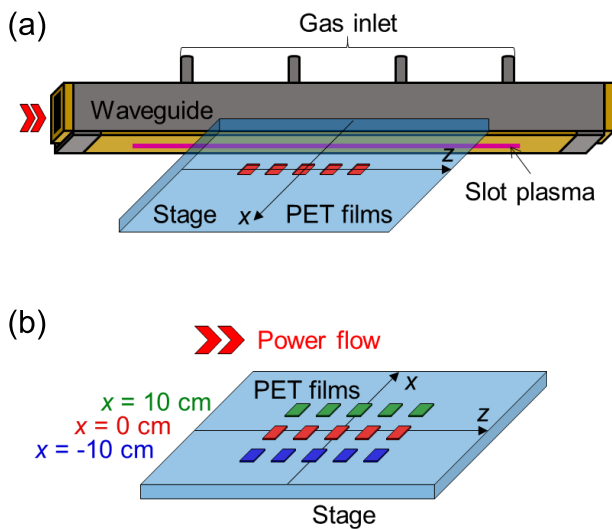


Fig. 8 Schematic image of (a) experimental setup for surface treatment of large surface area, and (b) substrate scanning stage.

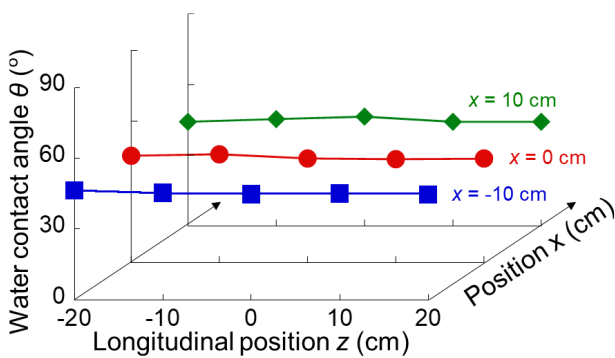


Fig. 9 Water contact angle of the PET film after Ar plasma treatment.

the treatment time by plasma irradiation, information on plasma-irradiation width is required. When the distance between the slot and the substrate is around 1.5 mm, it is observed that plasma effusing from the slot tends to spread out to x direction. We have measured the spread plasma using a digital still camera through a glass substrate and have estimated the spread width in the x direction to be around 0.8 mm in FWHM. From the scanning speed and the plasma width in the x direction, the treatment time is obtained. Figure 10 shows the water contact angle as a function of the treatment time, where treatment time is varied by changing the scanning speed of the stage. As the treatment time increases, the water contact angle monotonically decreases and reaches its saturated value (35°) at treatment times above 50 ms. So far various surface treatment experiments were reported [27–32] and the present result shows fairly high treatment speed compared with previous results. It should also be noted that the APMLP can be used in wide-area surface treatment, in contrast with

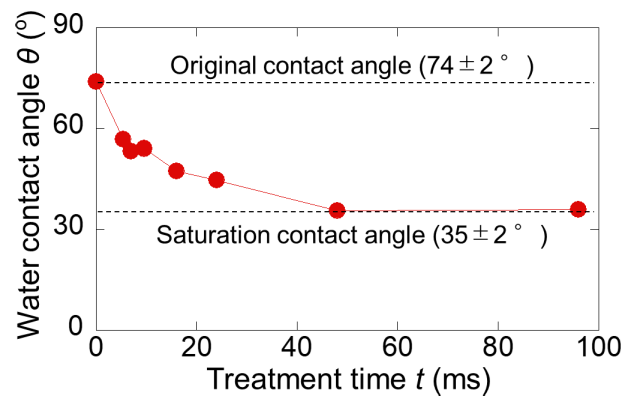


Fig. 10 Water contact angle of the PET film as a function of the treatment time.

previous reports in which APP was used in the treatment of small surface areas.

The following mechanisms for hydrophilization of the film surface have been proposed. The first is that the surface intermolecular bonds are cleaved by irradiation with charged particles, reactive species derived from ambient air and ultraviolet rays from plasma, and hydrophilic functional groups such as OH, CO, and COOH, are formed to increase hydrophilicity. The second is that the surface area is increased by the surface roughness due to plasma irradiation, which improves the adhesiveness with water. In the experiment, the distance between sample slots is set to 1.5 mm. Other experiments revealed that there is a strong dependence on the distance and the hydrophilicity is further improved by adding a small amount of molecular gas to Ar gas. Since the surface of the treated sample has not been analyzed, the details are not clear, but we consider that the reactive species are uniformly transported over a long length from the plasma to the PET film and contribute to improving hydrophilicity, because reactive species are easily deactivated in the atmosphere due to the short mean free path.

5. Conclusion

Spatial uniformity of an atmospheric-pressure microwave line plasma is evaluated from surface hydrophilicity treatment of PET film as well as observation of optical emission from the plasma. Prior to the experiments, the structure of the waveguide-based plasma source is optimized using a three-dimensional electromagnetic simulation to suppress standing-wave generation for the uniformity of plasma production. The spatial distribution in the longitudinal direction of the plasma is investigated by operating the microscope parallel to the slot. The emission intensity is slightly high at the upstream side of the microwave power flow. However, the difference of the emission intensity at $z = -30$ cm and $z = +30$ cm is within 6%. It is confirmed that one-dimensional uniform plasma

is produced along the slot with a length of 60 cm. To demonstrate the potential of the APMLP for use in the surface treatment of large surface areas, PET film is irradiated with the Ar plasma to improve the surface wettability. Uniform distribution is obtained in 40 cm with very high-speed processing.

Acknowledgments

This work was supported by JSPS KAKENHI JP18K13531.

- [1] M. Iwasaki *et al.*, Appl. Phys. Lett. **92**, 081503 (2008).
- [2] M.J. Shenton and G.C. Stevens, J. Phys. D: Appl. Phys. **34**, 2761 (2001).
- [3] M.J. Shenton *et al.*, J. Phys. D: Appl. Phys. **34**, 2754 (2001).
- [4] M. Noeske *et al.*, Int. J. Adhes. Adhes. **24**, 171 (2004).
- [5] R. Foest *et al.*, Plasma Phys. Control. Fusion **47**, B525 (2005).
- [6] Y. Sawada *et al.*, J. Phys. D: Appl. Phys. **29**, 2539 (1996).
- [7] Y. Sawada *et al.*, Jpn. J. Appl. Phys. **38**, 6506 (1999).
- [8] Y. Mori *et al.*, Rev. Sci. Instrum. **71**, 3173 (2000).
- [9] N. Gherardi, S. Martin and F. Massines, J. Phys. D: Appl. Phys. **33**, L104 (2000).
- [10] Y. Ito, O. Sakai and K. Tachibana, Thin Solid Films **518**, 3513 (2010).
- [11] T. Belmonte *et al.*, J. Therm. Spray Technol. **20**, 744 (2011).
- [12] M. Agemi *et al.*, Surf. Coat. Technol. **206**, 2025 (2011).
- [13] U. Kogelschatz, Plasma Chem. Plasma Process. **23**, 1 (2003).
- [14] F. Massines *et al.*, Plasma Phys. Control. Fusion **47**, B577 (2005).
- [15] A. Schutze *et al.*, IEEE Trans. Plasma Sci. **26**, 1685 (1998).
- [16] N. Balcon *et al.*, Plasma Sources Sci. Technol. **16**, 217 (2007).
- [17] M. Laroussi and T. Akan, Plasma Process. Polym. **4**, 777 (2007).
- [18] M. Moisan *et al.*, Plasma Sources Sci. Technol. **3**, 584 (1994).
- [19] A. Kono *et al.*, Jpn. J. Appl. Phys. **40**, L238 (2001).
- [20] Y. Kabouzi *et al.*, J. Appl. Phys. **91**, 1008 (2002).
- [21] H. Itoh *et al.*, Jpn. J. Appl. Phys. **52**, 11NE01 (2013).
- [22] K. Sasai *et al.*, Jpn. J. Appl. Phys. **57**, 066201 (2018).
- [23] H. Suzuki *et al.*, Appl. Phys. Express **8**, 036001 (2015).
- [24] H. Suzuki *et al.*, Jpn. J. Appl. Phys. **55**, 01AH09 (2016).
- [25] H. Suzuki and H. Toyoda, Jpn. J. Appl. Phys. **56**, 116001 (2017).
- [26] H. Suzuki *et al.*, Jpn. J. Appl. Phys. **59**, 016002 (2020).
- [27] K. Navaneetha Pandiyaraj *et al.*, Vacuum **83**, 332 (2009).
- [28] C. Huang *et al.*, Thin Solid Films **518**, 3575 (2010).
- [29] Z. Fang *et al.*, IEEE Trans. Plasma Sci. **41**, 1627 (2013).
- [30] W.S. Kang *et al.*, Appl. Surf. Sci. **295**, 198 (2014).
- [31] F.E. Wiria *et al.*, J. Solid State Electrochem. **20**, 1895 (2016).
- [32] F. Rezaei *et al.*, Surf. Coat. Technol. **309**, 371 (2017).